Photophysical and Theoretical Investigations of Oligo(*p*-phenyleneethynylene)s: Effect of Alkoxy Substitution and Alkyne−Aryl Bond Rotations

P. V. James,[†] P. K. Sudeep,[†] C. H. Suresh,*[,‡] and K. George Thomas*[,†]

Photosciences and Photonics, Chemical Sciences Division, and Computer Simulations and Modeling Group, Regional Research Laboratory (CSIR), Trivandrum 695 019 India

Received: September 14, 2005; In Final Form: January 14, 2006

The unique photophysical, conformational, and electronic properties of two model phenyleneethynylene-based rigid rod molecular systems, possessing dialkoxy substitutions, are reported in comparison with an unsubstituted system. Twisting of the phenyl rings along the carbon−carbon triple bond is almost frictionless in these systems giving rise to planar as well as several twisted ground-state conformations, and this results in broad structureless absorption in the spectral region of 250−450 nm. In the case of 1,4-bis(phenylethynyl)-benzene, a broad absorption band was observed due to the HOMO−LUMO transition, whereas dialkoxy-substituted compounds possess two well-separated bands. Dialkoxy substitution in the 2,5-position of the phenyl ring in phenyleneethynylenes alters its central arene π-orbitals through the resonance interaction with oxygen lone pairs resulting in similar orbital features for HOMO and HOMO−1/HOMO−2. Electronic transition from the low-lying HOMO−1/HOMO−2 orbital to LUMO results in the high-energy band, and the red-shifted band originates from the HOMO−LUMO transition. The first excited-state transition energies at different dihedral angles, calculated by the TDDFT method, indicate that the orthogonal conformation has the highest excitation energy with an energy difference of 15 kcal/mol higher than the low-lying planar conformation. The emission of these compounds originates preferentially from the more relaxed planar conformation resulting in well-defined vibronic features. The fluorescence spectral profile and lifetimes were found to be independent of excitation wavelengths, confirming the existence of a single emitting species.

Introduction

Newer synthetic strategies based on Sonogashira cross-coupling reaction[1] and its modifications have provided numerous possibilities for the design of rigid molecular systems based on phenylethynyl spacer groups. Such molecular systems possess a well-defined architecture and are widely used in the design of functional molecular materials such as conjugated polymers,[2−12] donor−acceptor systems,[13−21] sensors,[22−30] and self-assembled monolayers on metal surfaces.[31−34] The major advantage of using the oligo(phenyleneethynylene) core unit as a bridge for electronic communication may be attributed to the cylindrical symmetry of the acetylene unit which maintains the π-electron conjugation at any degree of rotation. Although a variety of phenylethynyl-based molecular systems have been investigated, most of the photophysical reports are based on unsubstituted 1,4-bis(phenylethynyl)benzene (**1** in Chart 1).[35−38]

The rotation of the central arene ring of this system revealed a very shallow potential of 0.5 kcal/mol between the fully planar and perpendicular structures.[35] It is also reported that **1** exists as a single species in the excited state and the photoexcitation does not bring about any significant changes in the bond order of the acetylene group, ruling out any cumulenic/quinanoidal character in its singlet excited state (S_1).[37,38] Oligo(phenyleneethynylene)s, particularly their higher analogues, possess poor solubility, which is one of the major limiting factors in the design of organic molecular materials. To overcome the solubility problem, 2,5-dialkoxy-substituted derivatives of oligo(phenyleneethynylene)s have been synthesized, and these molecular systems are widely used as building blocks for various functional molecular materials. However, the introduction of such groups with a lone pair of electrons can influence the photophysical properties of phenylethynyl-based systems, and detailed experimental as well as theoretical understanding is essential for fine-tuning their optoelectronic properties. With this objective, we have synthesized two model oligo(phenyleneethynylene)s possessing dialkoxy substitution, namely, 1,4-bis(phenylethynyl)-2,5-bis(hexyloxy)benzene (**2**)[39] and 1,4-bis-((4-phenylethynyl)phenylethynyl)-2,5-bis(hexyloxy)benzene (**3**) (Chart 1) and investigated their ground- and excited-state properties in detail. Further, DFT (density functional theory) and TDDFT (time-dependent density functional theory) levels of theoretical studies were carried out to understand the

CHART 1: Phenylethynyl-Based Molecular Systems under Investigation

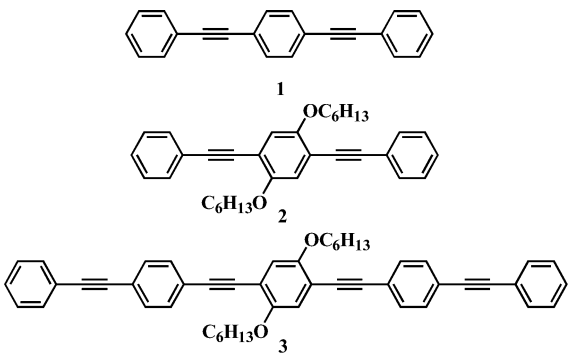

* Corresponding authors. E-mail: sureshch@gmail.com (C.H.S.); georgetk@md3.vsnl.net.in (K.G.T.).
[†] Chemical Sciences Division.
[‡] Computer Simulations and Modeling Group.

10.1021/jp055184o CCC: $33.50
Published on Web 03/11/2006

SCHEME 1: Synthetic Route for the Preparation of 2 and 3[a]

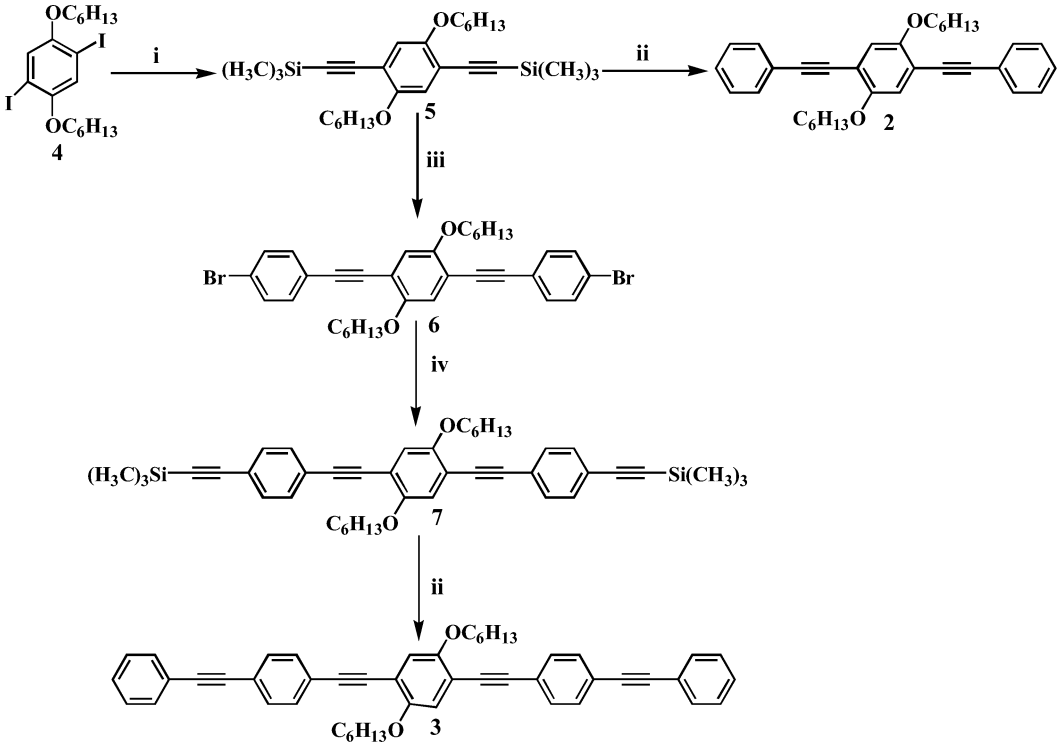

[a] (i) (Trimethylsilyl)acetylene, $Pd(PPh_3)_2Cl_2$, CuI, $(i\text{-pr})_2NH$, 80 °C, 1 h; (ii) CH_3OH, K_2CO_3, THF, C_6H_5I, $Pd(PPh_3)_4$, CuI, PPh_3; (iii) CH_3OH, K_2CO_3, THF, BrC_6H_4I, $Pd(PPh_3)_4$, CuI, PPh_3; (iv) (trimethylsilyl)acetylene, $Pd(PPh_3)_2Cl_2$, CuI, $(i\text{-pr})_2NH$, 80 °C, 3 h.

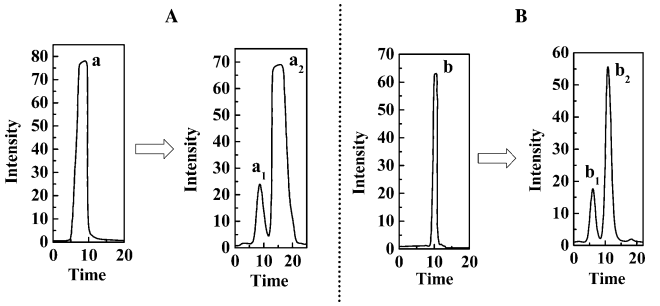

Figure 1. Chromatograms of phenyleneethynylenes obtained in the first cycle (peaks "a" and "b") and after recycling (peaks "a_1" and "b_1" are impurities and "a_2" and "b_2" are purified products) through HPLC: (A) compound **2** was recycled 17 times and (B) compound **3** was recycled 14 times.

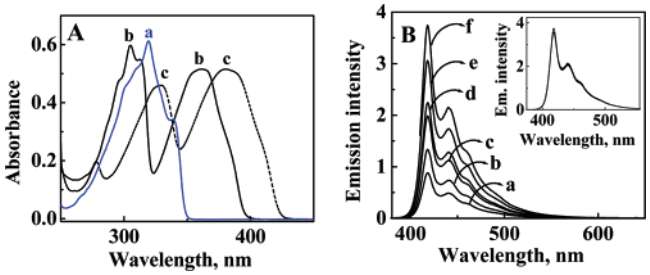

Figure 2. (A) Absorption spectrum of phenyleneethynylenes in methylcyclohexane: (trace a) **1**; (trace b) **2**; (trace c) **3**. (B) Fluorescence emission spectra of **3** in methylcyclohexane on exciting at (trace a) 310, (trace b) 320, (trace c) 340, (trace d) 350, (trace e) 375, and (trace f) 400 nm. The inset in (B) shows the normalized emission spectrum of **3** at different exciting wavelengths.

conformational, electronic, and excited-state properties of **2** and **3** in comparison with those of **1**.

Results and Discussion

The general strategy adopted for the synthesis of compounds **2** and **3** is shown in Scheme 1 (an alternate route for the synthesis of **2** is reported in ref 39). It is important to note that it was somewhat difficult to separate the trace amounts of impurities present in **2** and **3** using conventional column chromatographic or crystallization techniques. To ensure high purity of the samples used in the photophysical studies, compounds were further purified by using recycling HPLC[40] with two columns connected in series. Typically 20−30 mg of phenyleneethynylenes, dissolved in chloroform (3 mL), was injected and eluted using the same solvent. Effective removal of even trace amounts of impurities could be achieved by recycling the samples for about 14−20 cycles. Figure 1 shows the chromatograms of phenyleneethynylenes obtained in the first cycle (peaks "a" and "b") and after recycling through HPLC. Peaks "a_2" and "b_2" in Figure 1 corresponds to compounds **2** and **3** which were further characterized by various analytical and spectroscopic techniques (Experimental Section).

Photophysical Investigation. The absorption spectral feature of **1**, shown in Figure 2A (trace "a"), was earlier reported by several groups as a broad band (partially resolved) in the spectral region of 250−350 nm.[35−38] In contrast, the absorption spectra of **2** and **3** recorded in different solvents (methylcyclohexane, toluene, and dichloromethane) showed significantly different features with two well-separated bands. For example, the spectrum of **2** in methylcyclohexane possess a shorter wavelength band between 275 and 325 nm, with partially resolved vibronic features, and a long wavelength band with a maximum around 367 nm of almost the same intensity (trace "b" in Figure 2A). In an earlier report, Li et al. have reported the absorption spectra of **2** with similar spectral features.[39] In the case of **3**, both the absorption bands are red shifted by around 20 nm due to the increase in conjugation; however, they do not possess any distinct vibronic features. From these studies it is obvious that the dialkoxy substitution has a significant effect on the photophysical properties of phenyleneethynylenes. The splitting

TABLE 1: Stokes Shift ($\nu_{abs} - \nu_{em}$) and Fluorescence Lifetimes (τ_f) of 2 and 3 in Different Solvents[a,b]

	compound **2**		compound **3**	
solvent	$(\nu_{abs} - \nu_{em})$ $(cm^{-1})^a$	τ_f $(ns)^b$	$(\nu_{abs} - \nu_{em})$ $(cm^{-1})^a$	τ_f $(ns)^b$
methylcyclohexane	2130	1.28	2500	0.88
toluene	2130	1.37	2300	1.10
dichloromethane	2000	1.50	2200	1.01

[a] $(\nu_{abs} - \nu_{em})$, Stokes shift. [b] τ_f, fluorescence lifetime (error limit ± 5%).

of the absorption band observed for **2** and **3** compared to **1** is discussed in detail using theoretical studies (vide infra). The absorption spectral profiles of **2** and **3** remain unaffected with increase in concentration (up to 15 μM) and were found to be independent of the nature of the solvent (Supporting Information), ruling out the possibility of any ground-state interactions such as aggregation. The fluorescence spectra of **2** and **3** were recorded by exciting at different wavelengths, ranging from 290 to 400 nm, in three different solvents. A representative example (**3** in methylcyclohexane) is presented in Figure 2B and the others under the Supporting Information. In all the cases, the absorbance of the solution was kept as 0.1 at the excitation wavelength. The emission spectra of **3**, in methylcyclohexane, obtained by exciting at different wavelengths were normalized and presented in the inset of Figure 2B. In contrast to the absorption spectra, the emission spectra of both the compounds possess well-structured vibronic bands in methylcyclohexane, indicating that the excited-state geometry of phenyleneethynylenes is more planar compared to that of the ground state. These aspects were further confirmed by calculating the excited-state energy barrier using theoretical methods (vide infra). The vibronic features of the normalized emission spectra were found to be identical on exciting at different wavelengths (Figure 2B) indicating the presence of a single emitting species. The emission spectra were further compared in methylcyclohexane, toluene, and dichloromethane. Vibronic features in dichloromethane are less distinct compared to those in methylcyclohexane, and no appreciable change in the spectral features was observed on varying the solvent polarity. The Stokes shifts of phenyleneethynylenes **2** and **3** were calculated as ~2100 and ~2300 cm^{-1} (Table 1). The Stokes loss reported for rigid aromatic molecules such as fluorine is ~1430 cm^{-1} and that of biphenyls which undergo conformational change in the excited state leading to planarization in the excited state is ~3310 cm^{-1}.[41] The intermediate values obtained for **2** and **3** suggest that these compounds undergo conformational changes in the excited state favoring a more stable planar conformation. On the basis of theoretical investigation it is confirmed that the rotational energy barrier of the arene rings along the molecular axis must be higher in the excited state, and this limits the number of conformers leading to a structured emission (vide infra). Fluorescence excitation spectra of **2** and **3** were recorded by collecting the emission at three different wavelengths and resemble the UV−vis absorption spectrum (Supporting Information).

To further confirm the presence of a single emitting species in the excited state, detailed fluorescence lifetime studies of **2** and **3** were carried out using single-photon counting technique at different excitation wavelengths and solvent polarities. Fluorescence lifetimes (τ_f) of **2** and **3** in different solvents are summarized in Table 1. The compounds were excited at 280, 375, and 394 nm, and the emission was collected at different wavelengths. In a particular solvent system, fluorescence lifetime (τ_f) was found to be independent of the excitation wavelength and the wavelength at which the emission is collected. In all the cases, emission decay exhibited monoexponential decay further confirming the presence of a single emitting species, and the details are presented in the Supporting Information.

Theoretical Investigations. Various conformations of phenyleneethynylene-based rigid rod molecular systems (**2** and **3** in Chart 1) were optimized at the AM1 level, a semiempirical method widely used for obtaining reliable geometries for organic systems. Highest and lowest energy conformations derived from AM1 level calculations were further optimized by the B3LYP/6-31G* level density functional theory (DFT) method.[42,43] In the DFT method, electron correlation effects were taken into account, and this method is often used as a compromise for higher end calculation at a reasonable computational cost.[44,45] The basic photochemical properties of these systems were investigated by means of quantum chemical calculations employing mainly the time-dependent density functional theory (TDDFT) formalism[46−48] as well as Zerner's intermediate neglect of differential overlap (ZINDO/S) method.[49,50] TDDFT using B3LYP input has been proved to be more accurate for many molecular systems including poly(phenylenevinylyne) (PPV) type polymers.[51] For all the calculations, the Gaussian03[52] suite of programs was used.

A detailed ground-state conformational analysis of **2** and **3** was carried out using the AM1 semiempirical quantum mechanical method. The stationary points thus obtained were confirmed as minima by performing normal coordinate analysis. The main focus of the present investigation is to understand the conformational, π-conjugation, and excited-state properties of phenylethynylenes **2** and **3**, in comparison with those of the unsubstituted compound **1**. A completely planar geometry (**1a**) is the only minimum energy conformation for **1** wherein one π-bond from each of the acetylene units conjugates with 18 π-electrons from the three benzenoid rings resulting in an extended π-conjugation. In contrast, four different minimum energy conformations have been obtained for **2** and **3**. The conformations obtained for **2** are depicted in Figure 3, and conformations of **3**, namely, **3a**, **3b**, **3c**, and **3d** are presented under the Supporting Information. In the most stable conformation of **2** and **3** (i.e., **2a** in Figure 3 and **3a** in the Supporting Information), the alkoxy chain and the benzenoid rings occupy the same plane leading to maximum resonance interaction between the oxygen lone pairs and the arene ring π-electrons. In the next lower energy conformation (**2b** and **3b**), one alkoxy chain remains in the benzenoid plane and the other one is twisted out of the plane. Both the alkoxy groups are twisted out to opposite sides of the benzenoid plane in the third conformer (**2c** and **3c**), while in the forth conformer (**2d** and **3d**), both substituents are twisted out to the same side of the plane.

Starting from the most stable trans in-plane conformation of compound **2** and **3** (**2a** in Figure 3 and **3a** in the Supporting Information), the rotation of the phenyl groups along the triple bond is modeled. In the case of conformation **2a**, the rotation of the central phenyl ring with respect to the terminal ones is modeled by constraining the angle between the planes of the central and the terminal rings to the increments of 10°. The conformer with highest heat of formation corresponds to the one with the central and terminal rings are orthogonal. This orthogonal conformation is found to 0.6 kcal/mol less stable than the fully planar structure **2a**. Further, by constraining the angle made by the terminal phenyl rings, one more conformation is obtained in which the terminal rings are orthogonal and the angle between the center and terminal ring planes is 45°. The energy required for such a twisting is only 0.3 kcal/mol. Several

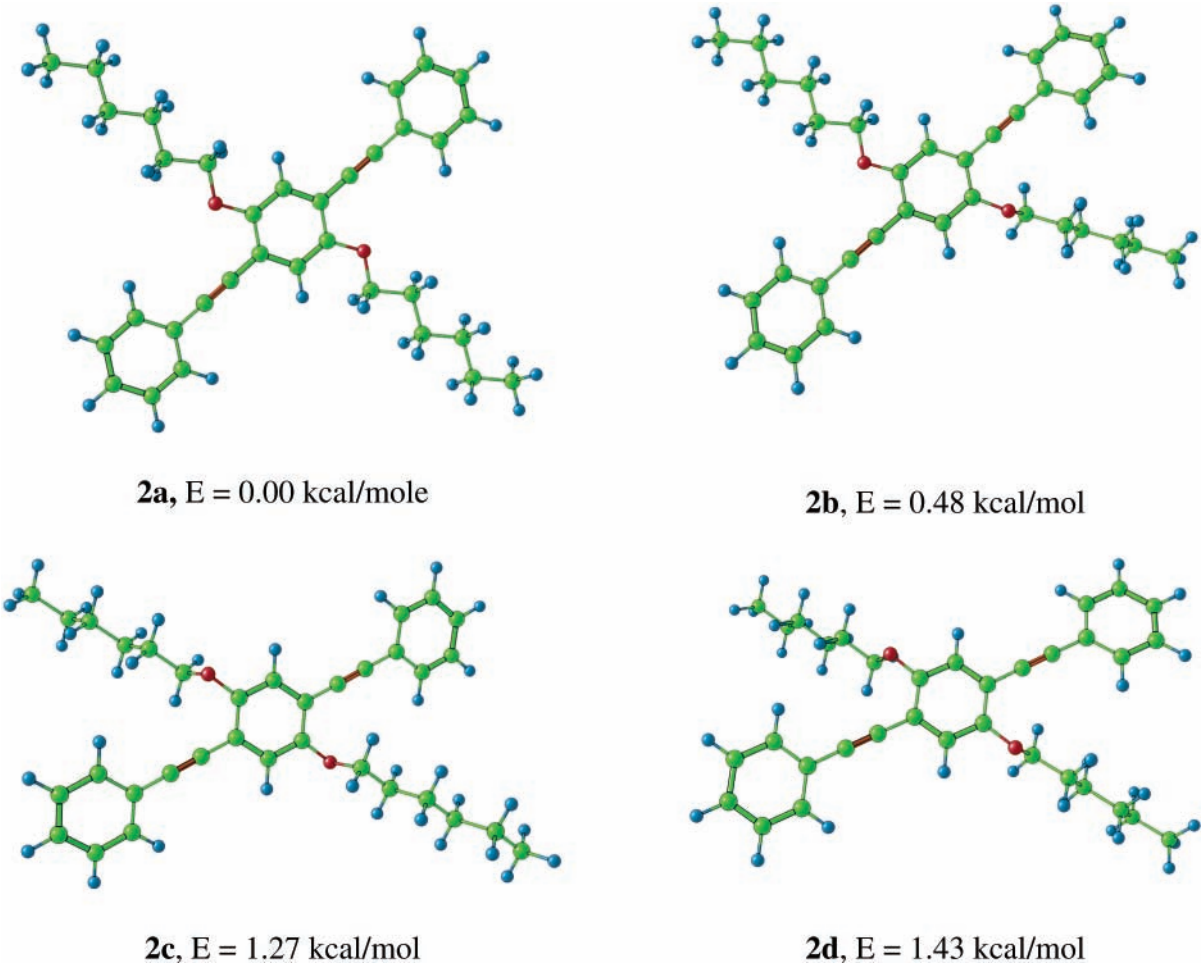

Figure 3. Four different conformers of **2** obtained by AM1 semiempirical calculations and their relative heats of formation. Conformations of **3**, namely, **3a**, **3b**, **3c**, and **3d** are presented in the Supporting Information.

twisted conformations are possible in the case of **3** due to the presence of five phenyl rings, and some of these optimized structures are presented in the Supporting Information. A conformer in which all the adjacent phenyl rings are orthogonal to each other showed the highest heat of formation, interestingly even this conformer was only 1 kcal/mol less stable than the planar conformer.

The most stable and the least stable structures at the AM1 level were further optimized at the B3LYP/6-31G* level of density functional theory. To reduce the computational cost, the hexyloxy substituents were replaced with ethyloxy substituents and the corresponding compounds were named as **2′** and **3′**. The structures optimized using AM1 and those obtained by DFT showed only little difference from the X-ray structure reported.[39] However, a more refined geometry in terms of bond angles and C−O bond distances were obtained by the DFT level of optimization. For example, in the case of **2′** the O−C(sp^3, alkyl)−C(sp^3, alkyl) bond angle in the alkoxy side chain is calculated to be 107.4° by DFT which is only 0.28° higher than that in the X-ray structure, while the AM1 calculations provided a lower value of 105.6°. Similarly, in the DFT level of optimization the C(sp^2, arene)−O bond distance showed a negligible difference of only 0.005 Å less than the X-ray structure. The most stable and the least stable optimized geometries of phenyleneethynylenes **1**−**3** and their relative energies are depicted in Figure 4. The structures and the relative energies of the other conformations are presented in the Supporting Information.

It can be seen from Figure 4 that the relative energy of **3′e** is 2 times larger compared to that of **2′e** since the number of orthogonal connections is double, and even at DFT level, there is only a difference of 4.8 kcal/mol between the most stable (**3′a**) and the least stable structures (**3′e**). This indicates that the twisting of phenyl rings along the carbon−carbon triple bond is almost frictionless, and one can expect planar as well as all sorts of twisted conformations for **1**, **2**, and **3** at room temperature. The small barrier of rotation for the phenyl rings can be easily explained from the features of the π-electron conjugation in these molecules. The planar conformation possesses a completely extended conjugation of the phenyl π-electrons through one of the π-bonds of each acetylenic bond. This smooth conjugation is broken at the orthogonal junctions in the perpendicular conformation, and the system loses some energy. However, this loss of energy is partially compensated by the participation of the second π-bond of the acetylenic bond. This feature of the π-electron conjugation can be visualized through their molecular electrostatic potential (MESP) distribution[53] as well as the relevant molecular orbitals as depicted in Figure 5.

With the use of the optimized planar geometries **1**, **2′a**, and **3′a** at the B3LYP/6-31G* level, the first 20 low-lying excited states have been calculated at the TDDFT and ZINDO/S levels. It is interesting to note that the unsubstituted phenyleneethynylene **1** possesses only one singlet state with significant oscillator strength, while **2′a**, and **3′a** showed two such states. These theoretical results are in good agreement with the number

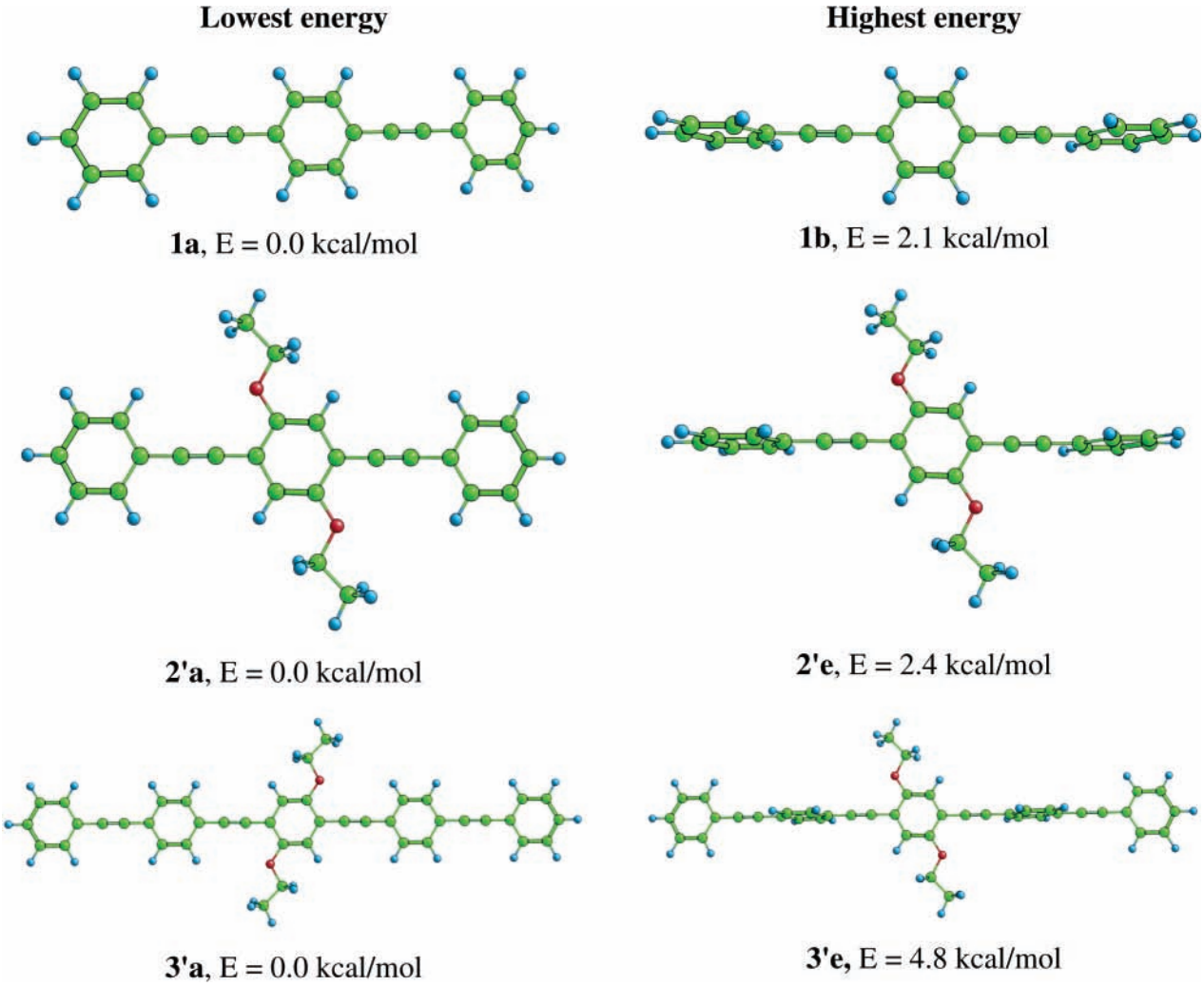

Figure 4. Most stable planar conformations and the least stable orthogonal conformations of phenyleneethynylenes **1**−**3** obtained by the B3LYP/6-31G* method and their relative energies.

of absorption peaks observed for **1**, **2**, and **3** (Figure 2A). The absorption wavelengths and the corresponding MOs involved were obtained by TDDFT and ZINDO/S methods and compared with experimental results (Table 2). The singlet excited state of **1** corresponds to the electronic transition from HOMO to LUMO (cf., Figure 6 for the orbitals), and the calculated wavelength of 360 nm (TDDFT) and 365 nm (ZINDO/S) for this absorption is in reasonable agreement with the experimental value of 320 nm (Figure 2A).

The TDDFT level calculated spectra and the corresponding MO transitions for **2′a** are given in Figure 7. A comparison of the MOs of the unsubstituted system in Figure 6 and those of **2′a** in Figure 7 suggest that the alkoxy substituent of **2′a** modifies its center arene ring π-orbitals through the resonance interaction with the oxygen lone pairs. This leads to the development of very similar orbital features for HOMO and HOMO−1 resulting in electronic transitions from both HOMO and HOMO−1 to LUMO for **2′a**. Similar orbital features are observed in **3′a** as well (details are provided in the Supporting Information). The calculated absorption maxima (λ_{cal}) are also in good agreement with the experimental values (λ_{exp}) in all three systems. In the case of **2′a** and **3′a**, the higher wavelength absorption corresponds to the electronic transition mainly from HOMO to LUMO (Table 2). The lower wavelength absorption originates from HOMO−1 to LUMO and HOMO−2 to LUMO for **2′a** and **3′a**, respectively. The orbital features of HOMO−1 of **2′a** and HOMO−2 of **3′a** are found to be similar, which implies the same type of electronic transition for lower wavelength absorptions.

Further the absorption wavelengths calculated using TDDFT and ZINDO/S methods were compared. For **2′a**, ZINDO/S calculations performed on the DFT-optimized structure provided a value of 379 nm (oscillator strength 1.199), closer to the experimental λ_{max} at 367 nm, whereas TDDFT gave the absorption wavelength as 393 nm (oscillator strength 1.343). In contrast, the absorption wavelength obtained for the short wavelength band by the TDDFT method (319 nm having an oscillator strength of 0.467) matched with the experimental λ_{max} (307 nm), while ZINDO/S delivered a much lower value of 268 nm with an oscillator strength of 0.247. For the long wavelength band of **3′a**, TDDFT showed a large deviation of 58 nm higher than the observed wavelength at 383 nm, while the ZINDO/S gave a comparable value of 406 nm. The short wavelength band of **3′a**, appeared at 330 nm, and the theoretical absorption wavelengths obtained by TDDFT and ZINDO/S are 357 and 331 nm, respectively. The deviations observed between the theoretical and experimental absorption maximum may be due to the influence of the solvent. The solvent molecules interacting at the acetylenic region can exert some steric effect, which would lead to some twisting of the arene rings, thereby reducing the degree of conjugation.

To understand the dependence of arene ring rotations of phenyleneethynylene on their electronic transition energies, a computational experiment was carried out on **2′a**. In this

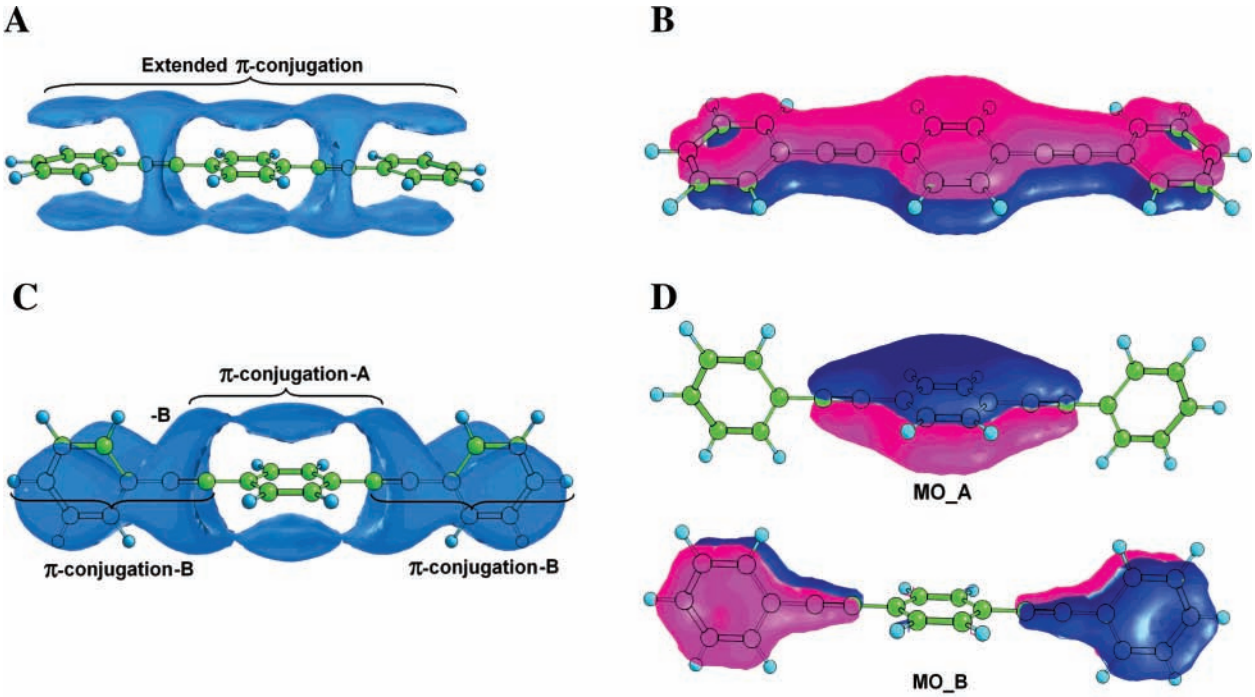

Figure 5. (A and C) show the π-conjugation features visualized through the molecular electrostatic potential isosurfaces with a value of −9.4 kcal/mol for **1a** and **1b**. (B) The molecular orbital showing the extended π-conjugation in **1a**. (D) The molecular orbitals MO_A and MO_B support the localized π-conjugations in **1b**.

TABLE 2: Experimental Wavelengths (λ_{exp}), Calculated Absorption Wavelengths (λ_{cal}), and Oscillator Strengths for 1−3[a,b]

			ZINDO/S		TDDFT	
compound	transition	exptl wavelength λ_{exp} (nm)[a]	λ_{cal} (nm)	oscillator strength	λ_{cal} (nm)	oscillator strength
1	HOMO to LUMO	320	365	1.304	360	1.897
2′	HOMO to LUMO	367	379	1.199	393	1.343
	HOMO−1 to LUMO	307	268	0.247	319	0.467
3′	HOMO to LUMO	383	406	2.413	461	2.951
	HOMO−2 to LUMO	330	331	0.284	357	0.443

[a] Figure 2A for **1** (ref 37), **2**, and **3**. [b] TDDFT and ZINDO/S level calculations using the B3LYP/6-31G* level optimized geometries of **1**, **2′**, and **3′**.

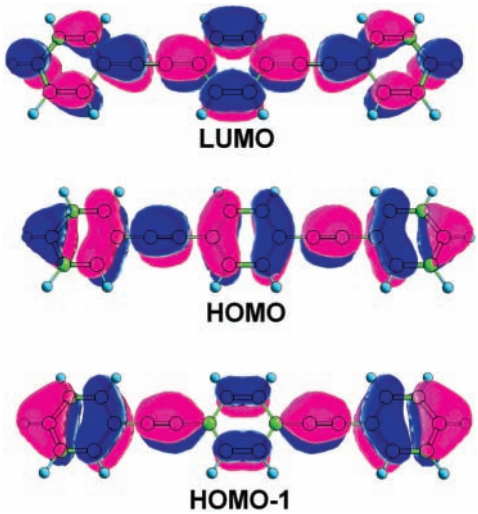

Figure 6. Frontier molecular orbitals of compound **1** obtained at the B3LYP/6-31G* level. The singlet excited state corresponds to the electron transition from HOMO to LUMO.

experiment, several rotamers of **2′a** are optimized at the B3LYP/6-31G* level by constraining the angle made by the central arene ring with the terminal ones at increments of 15°. For each rotamer thus obtained, the S_0-S_1 transition energy is calculated at the TDDFT level. The transition energies thus obtained plotted against the dihedral angle are presented in Figure 8. The orthogonal and the planar conformations show the highest and the lowest excitation energies, respectively. On the basis of the Franck−Condon principle, the transition energy difference between these two extreme conformations is taken as a measure of the rotational barrier. This rotational barrier between the planar and orthogonal conformations of **2′a** in its excited state turned out to be 15 kcal/mol at the TDDFT level and 9.9 kcal/mol using the ZINDO/S calculation. Phenyleneethynylenes relax from the high-energy orthogonal conformation to the low-lying planar conformation, and the emission of the molecules is preferentially from the more planar structures resulting in the structured emission spectrum. The energy values and the oscillator strength in the excited state corresponding to transition from each geometry are given in the Supporting Information. This type of relaxation phenomena has been well documented without any ambiguity in oligo(phenylenevinylynes) (OPV) systems.[54−56] The ground-state structure of OPV is not planar; on excitation it undergoes a conformational change from the twisted ground-state geometry to planar conformation, and the emission is from the more planar conformation.[54] The extent of planarization in OPV mainly depends on the substitution on the vinylic carbons and on the phenyl ring.[55] Another feature

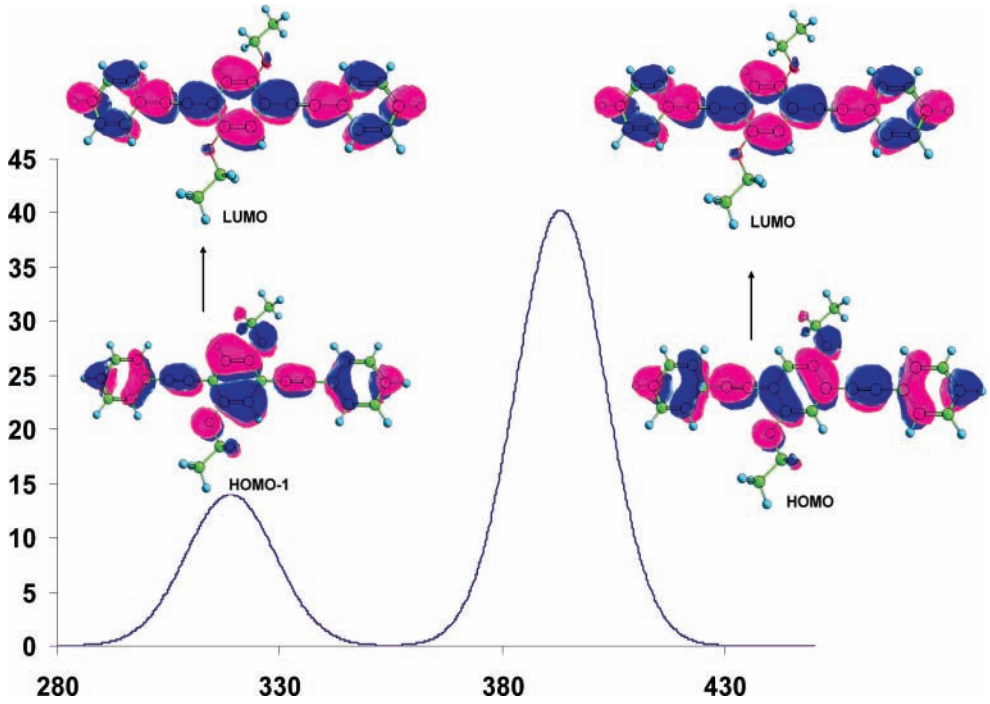

Figure 7. Absorption spectra calculated at the TDDFT B3LYP/6-31G* level for **2′a**. The important MO transitions corresponding to the peaks at 320 and 394 nm are also depicted.

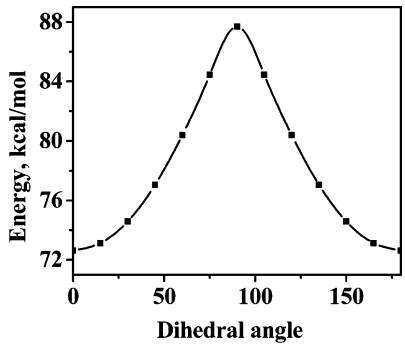

Figure 8. Transition energies for the first excited state of compound **2** obtained by the TDDFT level of calculation at different dihedral angles.

of OPV is the alteration of bond order in the excited state resulting in partial delocalization of the double bond throughout the system.[54,56]

Conclusions

We have synthesized two model phenyleneethynylene-based rigid rod molecules which are widely used as building blocks in various functional molecular materials and investigated their primary photophysical, conformational, and electronic properties. Purification of this class of molecules is rather difficult, and we successfully adopted recycling HPLC techniques. The photophysical and theoretical studies suggest that phenyleneethynylenes exist in planar and several twisted conformations in their ground state due to the nearly free rotation of the arene rings along the molecular axis. On the other hand, their emission spectra are highly structured as a consequence of the planarization of the molecules in the excited state. An idealized representation for the ground and excited states of a model phenyleneethynylene is shown in Scheme 2.

The emission properties and lifetimes of both the compounds were found to be independent of excitation wavelengths and solvent polarity, further confirming the existence of a single

SCHEME 2: Idealized Representation of the Ground and Excited States of Model Phenyleneethynylenes

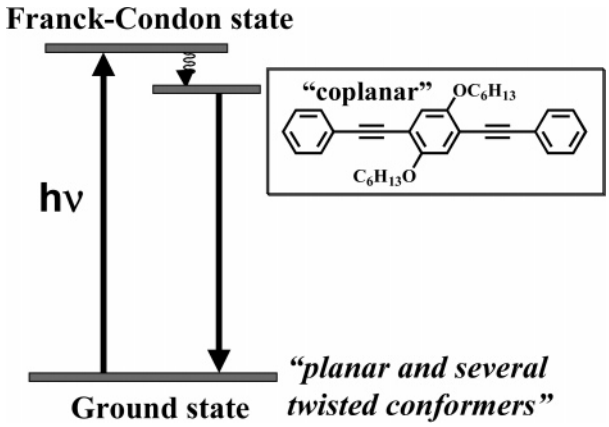

emitting species. The TDDFT results were found to be valuable for assigning the effect of alkoxy substituents on the absorption properties of **2** and **3**. The two distinct bands in the absorption spectra of **2** and **3** are due to the electronic transitions from nearly identical HOMO and HOMO−1/HOMO−2 to LUMO.

Experimental Section

Materials and Methods. The samples used for the study were purified by passing through recycling HPLC manufactured by Japan Analytical Industry Co., Ltd. All melting points are uncorrected and were determined on an Aldrich melting point apparatus. ^{1}H NMR and ^{13}C NMR spectra were recorded on a Bruker DPX-300 MHz spectrometer. High-resolution mass spectra were recorded on a JEOL JM AX 5505 mass spectrometer. The UV−vis spectra were recorded on a Shimadzu 2401 or 3101PC spectrophotometer. The emission spectra were recorded on a Spex-Fluorolog F112-X equipped with a 450 W Xe lamp and a Hamamatsu R928 photomultiplier tube. The spectra were recorded by keeping a 90° geometry and a band-pass of 1 nm in the excitation and emission monochromators.

Details of time-correlated single-photon counting fluorescence lifetime measurements were described earlier.[57]

General Method of Synthesis. Compounds **4** and **5** were prepared following the procedure reported in the literature.[39] Synthesis of **6** and **7** by an alternate route was reported by Xue and Luo.[58] THF used was dried over sodium, and diisopropylamine was dried over KOH. Solvents were deoxygenated by purging them with argon for 15 min, before using them in the reaction. The final compounds were purified by passing through recycling HPLC equipped with UV and RI detectors.

Preparation of 1,4-Bis(phenylethynyl)-2,5-bis(hexyloxy)-benzene (2). A mixture of TMS-coupled monomer **5** (500 mg, 1.06 mmol), K_2CO_3 (882 mg, 6.36 mmol), PPh_3 (111 mg, 0.106 mmol), $Pd(PPh_3)_4$ (245 mg, 0.053 mmol), CuI (40 mg, 0.053 mmol), and C_6H_5I (284 μL, 2.54 mmol) was stirred in a solvent mixture of CH_3OH/THF (1:4) at room temperature for 15 h. After removal of the solvent under reduced pressure, the crude product was purified by column chromatography over silica gel (100−200 mesh) using ethyl acetate/hexane (1:99) as eluent to yield 320 mg (63%) of white-colored product; mp 114−116 °C. ^{1}H NMR (300 MHz, $CDCl_3$): δ 7.54−7.52 (m, 4H), 7.35−7.33 (m, 6H), 7.02 (s, 2H), 4.03 (t, 4H), 1.87−0.87 (m, 22H). ^{13}C NMR (300 MHz, $CDCl_3$): δ 153.67, 131.568, 128.21, 128.22, 123.49, 117.07, 114, 94.82, 85.96, 77.42, 69.68, 31.60, 30.88, 29.33, 25.73, 22.62, 14.0. Anal. Calcd for $C_{34}H_{38}O_2$: C, 85.31; H, 8.00. Found: C, 85.55; H, 8.18. The exact mass calculated for $C_{34}H_{38}O_2$ ($M^{\bullet+}$) is 478.28719, found 478.28868 (FAB high-resolution mass spectrometry).

Preparation of 1,4-Bis(4-bromo-phenylethynyl)-2,5-bis-(hexyloxy)benzene (6). A mixture of TMS-coupled monomer **4** (500 mg, 1.06 mmol), K_2CO_3 (882 mg, 6.36 mmol), PPh_3 (111 mg, 0.106 mmol), $Pd(PPh_3)_4$ (245 mg, 0.053 mmol), CuI (40 mg, 0.053 mmol), and 1-bromo-4-iodo benzene (714 mg, 2.5 mmol) was stirred at room temperature in a solvent mixture of CH_3OH/THF (1:4) at room temperature for 15 h. The crude product was purified by column chromatography over silica gel (100−200 mesh) using ethyl acetate/hexane (1:19) as eluent to yield 460 mg (68%) of yellow solid; mp 112−114 °C. ^{1}H NMR (300 MHz, $CDCl_3$): δ 7.73−7.37 (m, 8H), 7.00 (s, 2H), 3.9 (t, 4H), 0.80−2.1 (m, 22H). ^{13}C NMR (300 MHz, $CDCl_3$): δ 153.63, 132.93, 131.59, 122.49, 122.38, 116.78, 113.82, 93.83, 87.08, 77.42, 77.00, 76.86, 76.58, 69.58, 31.56, 29.25, 25.715, 22.62, 14.01. Found *m*/*z* (FAB) 636.93; calcd 636.46.

Preparation of 1,4-Bis(hexyloxy)-2,5-bis((4-trimethylsilyl-ethynyl)phenylethynyl)benzene (7). To a stirring solution of aryl halide **6** (150 mg, 0.24 mmol), $Pd(PPh_3)_2Cl_2$ (16.5 mg, 0.024 mmol), and CuI (8.97 mg, 0.024 mmol) in 3 mL of diisopropylamine was added (trimethylsilyl)acetylene (75.5 μL, 0.29 mmol). The mixture was refluxed for 3 h under argon. After removal of the solvent, the crude product was crystallized using ethanol to give 64 mg (40%) of the product; mp 124−126 °C. ^{1}H NMR (300 MHz, $CDCl_3$): δ 7.37−6.9 (m, 10H), 4.02 (t, 4H), 1.9−0.9 (m, 11H). ^{13}C NMR (300 MHz, $CDCl_3$): δ 154.12, 131.85, 131.31, 116.84, 112.29, 77.42,77, 76.57, 69.6, 47.92, 29.27, 25.73, 22.62, 19.25, 14.01. Found *m*/*z* (FAB) 671.13; calcd 671.07.

Preparation of 1,4-Bis((4-phenylethynyl)phenylethynyl)-2,5-bis(hexyloxy)benzene (3). A mixture of **7** (300 mg, 0.45 mmol), K_2CO_3 (373.14 mg, 2.7 mmol), PPh_3 (47.16 mg, 0.18 mmol), $Pd(PPh_3)_4$ (104 mg, 0.09 mmol), CuI (17.1 mg, 0.09 mmol), and C_6H_5I (120.6 μL, 0.108 mmol) was stirred in a solvent mixture of CH_3OH/THF (1:4) at room temperature for 15 h. The crude product was purified by column chromatography over silica gel (100−200 mesh) using hexane/toluene (1:9) as eluent to yield 140 mg (46%) of yellow-colored solid; mp 173−175 °C. ^{1}H NMR (300 MHz, $CDCl_3$): δ 7.54−7.51 (m, 12H), 7.54−7.51 (m, 6H), 7.01(s, 2H), 4.04 (t, 4H), 1.88−0.90 (m, 22H). ^{13}CNMR (300 MHz, $CDCl_3$): δ 131.61, 131.5, 131.47, 128.45, 123.1, 116.87, 113.96, 69.64, 31.6, 31.2277, 29.3, 25.75, 22.64, 14.03. Anal. Calcd for $C_{50}H_{46}O_2$: C, 88.46; H, 6.83. Found: C, 88.43; H, 7.17. The exact mass calculated for $C_{50}H_{46}O_2$ ($M^{\bullet+}$) is 678.34979, found 678.34968 (FAB high-resolution mass spectrometry).

Acknowledgment. We thank the Council of Scientific and Industrial Research (CSIR task force Project CMM 010) and the Department of Science and Technology, Government of India for financial support. We also thank Professor P. Natarajan and Professor P. Ramamurthy, National Centre for Ultrafast Processes and the Department of Inorganic Chemistry, University of Madras for allowing access to the Picosecond Time Correlated Single Photon Counting facilities. This is contribution No. RRLT-PPD-197 from the Regional Research Laboratory, Trivandrum, India.

Supporting Information Available: Absorption and emission spectra of **2** and **3** and their fluorescence lifetimes at different exciting wavelengths in different solvents; optimized geometries and their relative energies of **2** and **3**. This material is available free of charge via the Internet at http://pubs.acs.org.

References and Notes

(1) Bunz, U. H. F. *Chem. Rev.* **2000**, *100*, 1605.
(2) Breen, C. A.; Rifai, S.; Bulovic, V.; Swager, T. M. *Nano Lett.* **2005**, *5*, 1597.
(3) Nesterov, E. E.; Zhu, Z.; Swager, T. M. *J. Am. Chem. Soc.* **2005**, *127*, 10083.
(4) Englert, B. C.; Smith, M. D.; Hardcastle, K. I.; Bunz, U. H. F. *Macromolecules* **2004**, *37*, 8212.
(5) Funston, A. M.; Silverman, E. E.; Miller, J. R.; Schanze, K. S. *J. Phys. Chem. B* **2004**, *108*, 1544.
(6) Walters, K. A.; Ley, K. D.; Schanze, K. S. *Chem. Commun.* **1998**, 1115.
(7) Zhou, C.-Z.; Liu, T.; Xu, J.-M.; Chen, Z.-K. *Macromolecules* **2003**, *36*, 1457.
(8) Glusac, K. D.; Jiang, S.; Schanze, K. S. *Chem. Commun.* **2002**, 2504.
(9) Bangcuyo, C. G.; Ellsworth, J. M.; Evans, U.; Myrick, M. L.; Bunz, U. H. F. *Macromolecules* **2003**, *36*, 546.
(10) Jegou, G.; Jenekhe, S. A. *Macromolecules* **2001**, *34*, 7926.
(11) Hayashi, H.; Yamamoto, T. *Macromolecules* **1998**, *31*, 6063.
(12) Moroni, M.; Moigne, J. L. *Macromolecules* **1994**, *27*, 562.
(13) Yamaguchi, Y.; Tanaka, T.; Kobayashi, S.; Wakamiya, T.; Matsubara, Y.; Yoshida, Z.-I. *J. Am. Chem. Soc.* **2005**, *127*, 9332.
(14) Meier, H. *Angew. Chem., Int. Ed.* **2005**, *44*, 2482.
(15) Piotrowiak, P.; Galoppini, E.; Wei, Q.; Meyer, G. J.; Wiewior, P. *J. Am. Chem. Soc.* **2003**, *125*, 5278.
(16) Galoppini, E.; Guo, W.; Zhang, W.; Hoertz, P. G.; Qu, P.; Meyer, G. J. *J. Am. Chem. Soc.* **2002**, *124*, 7801.
(17) Dong, W.; Schlegel, J. M.; Galoppini, E. *Tetrahedron* **2002**, *58*, 5027.
(18) Hoertz, P. G.; Carlisle, R. A.; Meye, G. J.; Wang, D.; Piotrowiak, P.; Galoppini, E. *Nano Lett.* **2003**, *3*, 325.
(19) Meier, H.; Mühling, B.; Kolshorn, H. *Eur. J. Org. Chem.* **2004**, *69*, 1033.
(20) Wan, C.-W.; Burghart, A.; Chen, J.; Bergström, F.; Johansson, L. B.-Å.; Wolford, M. F.; GyumKim, T.; Topp, M. R.; Hochstrasser, R. M.; Burgess, K. *Chem. Eur. J.* **2003**, *9*, 4430.
(21) Koishi, K.; Ikeda, T.; Kondo, K.; Sakaguchi, T.; Kamada, K.; Tawa, K.; Ohta, K. *Macromol. Chem. Phys.* **2000**, *201*, 525.
(22) Wosnick, J. H.; Mello, C. M.; Swager, T. M. *J. Am. Chem. Soc.* **2005**, *127*, 3400.
(23) Pinto, M. R.; Schanze, K. S. *Proc. Natl. Acad. Sci. U.S.A.* **2004**, *101*, 7505−7510.
(24) Disney, M. D.; Zheng, J.; Swager, T. M.; Seeberger, P. H. *J. Am. Chem. Soc.* **2004**, *126*, 13343−13346.
(25) Wilson, J. N.; Bunz, U. H. F. *J. Am. Chem. Soc.* **2005**, *127*, 4124.

(26) Kim, I.-B.; Dunkhorst, A.; Gilbert, J.; Bunz, U. H. F. *Macromolecules* **2005**, *38*, 4560.
(27) Ulrich, G.; Ziessel, R. *Synlett* **2004**, 439.
(28) Murphy, C. B.; Zhang, Y.; Troxler, T.; Ferry, V.; Martin, J. J.; Jones, W. E., Jr. *J. Phys. Chem. B* **2004**, *108*, 1537.
(29) Metivier, R.; Amengual, R.; Leray, I.; Michelet, V.; Genet, J.-P. *Org. Lett.* **2004**, *6*, 739.
(30) Moon, J. H.; Deans, R.; Krueger, E.; Hancock, L. F. *Chem. Commun.* **2003**, 104.
(31) Hacker, C. A.; Batteas, J. D.; Garno, J. C.; Marquez, M.; Richter, C. A.; Richter, L. J.; van Zee, R. D.; Zangmeister, C. D. *Langmuir* **2004**, *20*, 6195.
(32) Stapleton, J. J.; Harder, P.; Daniel, T. A.; Reinard, M. D.; Yao, Y.; Price, D. W.; Tour, J. M.; Allara, D. L. *Langmuir* **2003**, *19*, 8245.
(33) Cai, L.; Yao, Y.; Yang, J.; Price, D. W., Jr.; Tour, J. M. *Chem. Mater.* **2002**, *14*, 2905.
(34) (a) Tour, J. M.; Jones, L.; Pearson, D. L.; Lamba, J. J. S.; Burgin, T. P.; Whitesides, G. M.; Allara, D. L.; Parikh, A. N.; Atre, S. V. *J. Am. Chem. Soc.* **1995**, *117*, 9529. (b) Hu, W.; Nakashima, H.; Furukawa, K.; Kashimura, Y.; Ajito, K.; Liu, Y.; Zhu, D.; Torimitsu, K. *J. Am. Chem. Soc.* **2005**, *127*, 2804.
(35) Levitus, M.; Schmieder, K.; Ricks, H.; Shimizu, K. D.; Bunz, U. H. F.; Garcia-Garibay, M. A. *J. Am. Chem. Soc.* **2001**, *123*, 4259.
(36) Li, H.; Powell, D. R.; Firman, T. K.; West, R. *Macromolecules* **1998**, *31*, 1093.
(37) (a) Beeby, A.; Findlay, K.; Low, P. J.; Marder, T. B. *J. Am. Chem. Soc.* **2002**, *124*, 8280. (b) Zhao, L.; Perepichka, I. F.; Türksoy, F.; Batsanov, A. S.; Beeby, A.; Findlay, K. S.; Bryce, M. R. *New J. Chem.* **2004**, *28*, 912.
(38) Beeby, A.; Findlay, K. S.; Low, P. J.; Marder, T. B.; Matousek, P.; Parker, A. W.; Rutter, S. R.; Towrie, M. *Chem. Commun.* **2003**, 2406.
(39) Li, H.; Powell, D. R.; Hayashi, R. K.; West, R. *Macromolecules* **1998**, *31*, 52.
(40) The recycling HPLC was manufactured by Japan Analytical Industry Co., Ltd. Two columns were employed to achieve effective separation of the impurities, the first column with an exclusion limit of 2×10^3 and the other with a limit of 1×10^3. Polystyrene was used as packing material in both columns. The retention period for compounds **2** and **3** was found to be 48−53 min and 42−48 min, respectively.
(41) Berlman, I. B. *Handbook of Fluorescence Spectra of Aromatic Molecules*, 2nd ed.; Academic Press: London, New York, 1971.
(42) Lee, C.; Yang, W.; Parr, R. G. *Phys. Rev. B* **1988**, *37*, 785−789.
(43) Becke, A. D. *J. Chem. Phys.* **1993**, *98*, 5648−5652.
(44) Norton, J. E.; Houk, K. N. *J. Am. Chem. Soc.* **2005**, *127*, 4162.
(45) Khuong, K. S.; Beaudry, C. M.; Trauner, D.; Houk, K. N. *J. Am. Chem. Soc.* **2005**, *127*, 3688.
(46) Stratmann, R. E.; Scuseria, G. E.; Frisch, M. J. *J. Chem. Phys.* **1998**, *109*, 8218.
(47) Bauernschmitt, R.; Ahlrichs, R. *Chem. Phys. Lett.* **1996**, *256*, 454.
(48) Casida, M. E.; Jamorski, C.; Casida, K. C.; Salahub, D. R. *J. Chem. Phys.* **1998**, *108*, 4439.
(49) Zerner, M. C.; Loew, G. H.; Kirchner, R. F.; Mueller, V. T. *J. Am. Chem. Soc.* **1980**, *102*, 589.
(50) Edwalds, W. D.; Zerner, M. C. *Theor. Chim. Acta* **1987**, *72*, 347.
(51) Yu, J. S. K.; Chen, W. C.; Yu, C. H. *J. Phys. Chem. A* **2003**, *107*, 4268.
(52) Frisch, M. J.; Trucks, G. W.; Schlegel, H. B.; Scuseria, G. E.; Robb, M. A.; Cheeseman, J. R.; Montgomery, J. A., Jr.; Vreven, T.; Kudin, K. N.; Burant, J. C.; Millam, J. M.; Iyengar, S. S.; Tomasi, J.; Barone, V.; Mennucci, B.; Cossi, M.; Scalmani, G.; Rega, N.; Petersson, G. A.; Nakatsuji, H.; Hada, M.; Ehara, M.; Toyota, K.; Fukuda, R.; Hasegawa, J.; Ishida, M.; Nakajima, T.; Honda, Y.; Kitao, O.; Nakai, H.; Klene, M.; Li, X.; Knox, J. E.; Hratchian, H. P.; Cross, J. B.; Adamo, C.; Jaramillo, J.; Gomperts, R.; Stratmann, R. E.; Yazyev, O.; Austin, A. J.; Cammi, R.; Pomelli, C.; Ochterski, J. W.; Ayala, P. Y.; Morokuma, K.; Voth, G. A.; Salvador, P.; Dannenberg, J. J.; Zakrzewski, V. G.; Dapprich, S.; Daniels, A. D.; Strain, M. C.; Farkas, O.; Malick, D. K.; Rabuck, A. D.; Raghavachari, K.; Foresman, J. B.; Ortiz, J. V.; Cui, Q.; Baboul, A. G.; Clifford, S.; Cioslowski, J.; Stefanov, B. B.; Liu, G.; Liashenko, A.; Piskorz, P.; Komaromi, I.; Martin, R. L.; Fox, D. J.; Keith, T.; Al-Laham, M. A.; Peng, C. Y.; Nanayakkara, A.; Challacombe, M.; Gill, P. M. W.; Johnson, B.; Chen, W.; Wong, M. W.; Gonzalez, C.; Pople, J. A. *Gaussian 03*, version 6.1; Gaussian, Inc.: Pittsburgh, PA, 2003.
(53) MESP is used widely for understanding molecular reactivity, intermolecular interactions, molecular recognition, electrophilic reactions, and a variety of chemical phenomena. For more details see: (a) Politzer, P.; Truhlar, D. G. *Chemical Applications of Atomic and Molecular Electrostatic Potentials*; Plenum: New York, 1981. (b) Gadre, S. R.; Shirsat, R. N. *Electrostatics of Atoms and Molecules*; Universities Press: Hyderabad, 2000; p 49. (c) Suresh, C. H.; Gadre, S. R. *J. Org. Chem.* **1999**, *64*, 2505−2512. (d) Suresh, C. H.; Koga, N.; Gadre, S. R. *J. Org. Chem.* **2001**, *66*, 6883−6890. (e) Suresh, C. H.; Koga, N. *J. Am. Chem. Soc.* **2002**, *124*, 1790−1797.
(54) Tretiak, S.; Saxena, A.; Martin, R. L.; Bishop, A. R. *Phys. Rev. Lett.* **2002**, *89*, 097402.
(55) Oelkrug, D.; Tompert, A.; Gierschner, D.; Egelhaaf, H.-J.; Hanack, M.; Hophloch, M.; Steinhuber, E. *J. Phys. Chem. B* **1998**, *102*, 1902.
(56) dos Santos, D. A.; Beljonne, D.; Cornil, J.; Bredas, J. L. *Chem. Phys.* **1998**, *227*, 1−10.
(57) Zeena, S.; Thomas, K. G. *J. Am. Chem. Soc.* **2001**, *123*, 7859.
(58) Xue, C.; Luo, F.-T. *Tetrahedron* **2004**, *60*, 6825.